A Trajectory Optimization Based Analysis of the 3Di Flight Efficiency Metric

Quintain McEnteggart
Cranfield University
Cranfield
Bedfordshire, MK43 0AL
Email: q.mcenteggart@cranfield.ac.uk

James Whidborne
Cranfield University
Cranfield
Bedfordshire, MK43 0AL
Email: j.f.whidborne@cranfield.ac.uk

***Abstract*—As a means of measuring progress towards fuel and emissions reduction targets, the United Kingdom Air Navigation Service Provider NATS developed the 3Di flight efficiency metric. In principle the 3Di score of a flight is calculated by comparing a flown trajectory to a theoretical fuel/CO2 optimum trajectory. In response to a Eurocontrol review of the metric, the 3Di score has been analysed using a trajectory optimization method based on optimal control. The results suggest that further development of the metric is required to make it sensitive to vertical flight inefficiencies not related to periods of level flight. The results also show that the BADA trajectories used in the 3Di score to define the optimum fuel efficient operation of the aircraft are not optimal fuel efficient trajectories. Additionally, the results show that fuel inefficiencies introduced by flight planning restrictions need to be accounted for in any vertical flight inefficiency metric.**

I. Introduction

Over the decade 2003 to 2013, global passenger air traffic increased by more than 70% [1]. Even factoring in the global economic downturn, continued high levels of traffic growth are projected for the coming decades [1], [2]. This growth however has come with an environmental cost. Increasing traffic levels, relying on greater consumption of fossil fuels, have led to increased levels of aircraft emissions, impacting climate change and local air quality [3]. Aviation's continued and rapid growth has seen it become the mode of transport with the fastest growing climate change impact [4], [5], [6]. Increasing traffic levels have also, despite an increasingly quiet aircraft fleet, led to an increase in the number of people exposed to significant levels of aircraft noise [7].

In Europe, the European Union market-based CO2 cap and trade system, the European Union Emissions Trading Scheme (EU ETS), included the aviation industry as of 2012 [8]. The aim of the inclusion is to incentivise CO2 related improvements in aircraft operations. In addition, a worldwide, CO2-based, aviation emissions trading scheme is being discussed by ICAO for implementation in 2020 [9], [10].

More long term strategic goals for CO2 reduction have been proposed by the Advisory Council for Aeronautics Research in Europe (ACARE) and the Single European Sky ATM Research (SESAR) programme for the years 2020 through to 2050. ACARE, a group of leading aviation stakeholders from industry, academia and the European Commission, have created the Strategic Research and Innovation Agenda (SRIA) [11], [12]. The SRIA is a high level roadmap for employing technology to meet the societal, economic, environmental and safety challenges facing the aviation industry in the coming decades. The ACARE goals are to be achieved through changes to aircraft airframes, engines and operational procedures. ACARE have proposed, from a 2000 baseline, a target of 10% improvement in the operational CO2 efficiency of flights [13].

Improving Air Traffic Management (ATM) related aircraft operations is the aim of SESAR, which is the research and development initiative of the Single European Sky (SES). Aligning with ACARE, the most specific environmental goal of SESAR is a 10% reduction in carbon dioxide emissions per flight (from a 2005 baseline) [14].

A. 3Di Score

As a means of measuring and managing progress towards fuel and emissions reduction goals, the 3D inefficiency (3Di) metric was developed by the United Kingdom Air Navigation Service Provider (ANSP) NATS. Specifically, the intention of the metric is to provide a measure of

- the flight efficiency of a flight [15],
- the fuel efficiency of a flight [16], [17],
- the environmental performance of a flight [18], [19],
- ANSP performance in delivering a preferred trajectory [17].

In principle, the 3Di score is calculated by comparing a flown trajectory to a theoretical fuel/CO2 optimum trajectory. Inefficiencies in the horizontal track and the vertical profile are measured independently and then combined into a weighted expression to determine the 3Di score of a flight. The theoretical optimal is defined as a totally environmentally efficient 4D trajectory that minimises fuel and therefore CO2 [20]. The long term use of the metric is intended to drive fuel burn and CO2 related improvements in trajectories [18].

To determine the coefficients used in the calculation of the 3Di score, the optimal vertical trajectory was defined by NATS as a BADA [21] generated trajectory along the great circle path between departure and arrival airports.

The BADA vertical trajectory was modelled using the standard BADA speed schedule as an uninterrupted climb and descent to and from a Requested Flight Level (RFL) and a cruise segment at the RFL. The fuel inefficiency for each trajectory within United Kingdom airspace was then determined

by comparing the fuel burn from a BADA generated trajectory (F_{REF}) to the estimated fuel burn from the actually flown trajectory (F_{ACT}) for a sample of 174,000 flights as

$$I = \frac{F_{ACT} - F_{REF}}{F_{REF}} \tag{1}$$

Using regression analysis, the fuel inefficiency I was further simplified to track extension distance σ to represent the horizontal inefficiency while time periods of level flight t_i below the RFL were used to calculate the vertical inefficiency.

The vertical inefficiency ν_i related to periods of level flight away from the BADA trajectory is then calculated as

$$\nu_i = \begin{Bmatrix} \frac{t_i(L-l_i)}{T_d L} & l_i \leq L \\ 0 & l_i > L \end{Bmatrix} \tag{2}$$

where l_i is the flight level during the level flight, T_d is the time duration of the flight and L is the Requested Flight Level (RFL) for the flight. It can be seen that periods above the RFL are regarded as having zero inefficiency. The inefficiency of periods of level flight below the RFL are calculated by multiplying the time duration by the difference between the actual flight level and the requested flight level. This acts to increase the vertical inefficiency value the lower the flown level flight level is from the RFL. To account for differing rates of fuel burn in different phases of flight, the vertical inefficiency is considered by phase of flight where

$$\nu_{CL} = \sum_{CLIMB} \nu_i, \quad \nu_{CR} = \sum_{CRUISE} \nu_i, \quad \nu_D = \sum_{DESCENT} \nu_i \tag{3}$$

and where the ν_{CL}, ν_{CR}, ν_D are the vertical inefficiency of the climb, cruise and descent phases respectively. The horizontal inefficiency part of the score, σ, is calculated by comparing the actual distance flown D_{ACT} to the minimum Great Circle Distance (GCD) that could have been flown between the same points D_{GCD}

$$\sigma = \frac{D_{ACT} - D_{GCD}}{D_{GCD}} \tag{4}$$

The differences between the distances are then considered to be the effect of fuel inefficiency introduced by tactical instructions, procedure and airspace design.

The 3Di inefficiency score ϑ is then determined by combining the horizontal and vertical inefficiencies into an overall inefficiency score

$$\vartheta = a_1\sigma + a_2\nu_{CL} + a_3\nu_{CR} + a_4\nu_D + a_5\nu_{CL}\sigma + a_6 v_{CR}\sigma + a_7\nu_D\sigma \tag{5}$$

where $a_1, a_2, a_3, a_4, a_5, a_6, a_7$ are 3Di score regression coefficients.

B. Metric Evaluation

In 2011 the UK CAA sought stakeholder consultation with regard to the 3Di metric [15]. Eurocontrol, the European organisation for the safety of air navigation responded as follows [22].

"Has NERL (NATS En Route Ltd) endeavoured to develop the best flight efficiency regime?, the answer would have to be in the negative; *there are no attempts to derive what the user considers to be the optimum flight profile beyond what is contained in the flight plan*, which is heavily influenced by vertical restrictions imposed at NERLs request. Moreover, the indicator is measured with reference to a model, which makes the indicator dependent on the validity of the model. Information on this model is too limited to take a view on its validity.

The horizontal flight efficiency appears straight forward and could certainly be applicable from 2012, being a variation (albeit considerable) of the KPI (Key Performance Indicator) established as part of the SES (Single European Sky) II Performance scheme. The vertical aspects are fundamentally different. *Considering the 2395 standing level agreements in the UK RAD (Route Availability Document), will these be considered as the optimum levels requested by the users or will these simply be removed from the vertical efficiency analysis?* If aircraft are subject to level capping then how will their optimum level be known to compare with the flight profile? The difference in profiles for these flights could be substantial and this will impact arriving traffic."

In summary, Eurocontrol questioned the optimality of the theoretical optimal trajectory and also highlighted the need for any vertical efficiency metric to consider the inefficiency introduced by flight planning restrictions [7].

C. Aims

In response to the Eurocontrol evaluation of the metric, the remainder of this paper will use a Inverse Dynamics trajectory optimization method to examine a number of aspects of the the 3Di score. Principally,

- the suitability of using level segments to define vertical fuel inefficiency,
- the suitability of using a BADA trajectory to define a fuel/CO2/environmentally optimal vertical trajectory,
- the effect of flight planning constraints on a fuel efficient trajectory.

II. Inverse dynamics method

The Inverse Dynamics in the Virtual Domain (IDVD) [23] method is a direct trajectory optimization method that has been previously applied to the calculation of environmentally efficient trajectories [24]. The method discretises the infinite dimensional optimal control problem and allows it to be treated as a finite dimensional Non Linear Programming (NLP) problem. As applied here, the method takes as input the desired aircraft position, speed and acceleration states at the start and end of the trajectory (t_o, t_f). It then determines the trajectory states $\mathbf{X}$ and controls $\mathbf{U}$ for $t \in [t_o, t_f]$ that minimise a

measure of performance J. In this paper, the performance measure adopted was the trajectory fuel burn

$$J = \int_{t_f}^{t_o} \dot{F}(\mathbf{X}(t), \mathbf{U}(t), t)dt \tag{6}$$

where $\dot{F}$ is the rate of fuel burn in in kilograms per second.

For the inverse method, the Cartesian positional states r_j $(j = 1, 2, 3)$ of the aircraft and their derivatives are parameterised with respect to the virtual arc τ by the reference function (7) and its derivatives.

$$r_j(\tau) = \sum_{k=0}^{7} \frac{a_{jk}\tau^k}{\max(1, k(k-1))} \tag{7}$$

For the virtual arc, derivatives of $(\cdot)$ with respect to τ are denoted $(\cdot)', (\cdot)'', etc.$ Time derivatives are denoted as $\dot{(\cdot)}, \ddot{(\cdot)}, etc.$ The coefficients of the reference polynomials defined by (7) are determined analytically from the coordinates and their derivatives at the boundaries ($\tau = 0$ and $\tau = \tau_f$) by making the coefficients the subjects of the following set of linear equations [25],

$$\mathbf{b}_j = \mathbf{C}\mathbf{a}_j, \ j = 1, 2, 3 \tag{8}$$

where $\mathbf{C}$ is a m by n matrix, $\mathbf{a}$ is a vector of polynomial coefficients and $\mathbf{b}$ is a vector of initial and final boundary conditions.

$$\mathbf{b}_j = \begin{bmatrix} r_{j0} \\ r'_{j0} \\ r''_{j0} \\ r'''_{j0} \\ r_{jf} \\ r'_{jf} \\ r''_{jf} \\ r'''_{jf} \end{bmatrix}, \quad \mathbf{a}_j = \begin{bmatrix} a_{j0} \\ a_{j1} \\ a_{j2} \\ a_{j3} \\ a_{j4} \\ a_{j5} \\ a_{j6} \\ a_{j7} \end{bmatrix},$$

$$\mathbf{C} = \begin{bmatrix} 1 & 0 & 0 & 0 & 0 & 0 & 0 & 0 \\ 0 & 1 & 0 & 0 & 0 & 0 & 0 & 0 \\ 0 & 0 & 1 & 0 & 0 & 0 & 0 & 0 \\ 0 & 0 & 0 & 1 & 0 & 0 & 0 & 0 \\ 1 & \tau_f & \frac{\tau_f^2}{2} & \frac{\tau_f^3}{6} & \frac{\tau_f^4}{12} & \frac{\tau_f^5}{20} & \frac{\tau_f^6}{30} & \frac{\tau_f^7}{42} \\ 0 & 1 & \tau_f & \frac{\tau_f^2}{2} & \frac{\tau_f^3}{3} & \frac{\tau_f^4}{4} & \frac{\tau_f^5}{5} & \frac{\tau_f^6}{6} \\ 0 & 0 & 1 & \tau_f & \tau_f^2 & \tau_f^3 & \tau_f^4 & \tau_f^5 \\ 0 & 0 & 0 & 1 & 2\tau & 3\tau^2 & 4\tau^3 & 5\tau^4 \end{bmatrix} \tag{9}$$

The coefficients of the reference polynomials are then determined analytically by inverting the matrix $\mathbf{C}$ and making $\mathbf{a}$ the subject of the linear equations $\mathbf{a}_j = \mathbf{C}^{-1}\mathbf{b}_j, \ j = 1, 2, 3$

Parameterising by τ adds an extra degree of freedom to the optimization and allows the speed profile to be optimized along the trajectory path of the aircraft. The relationship between the true airspeed v_t and the speed along the virtual arc $\sqrt{x'^2 + y'^2 + h'^2}$ is then defined as

$$v_\mathrm{t} = \lambda\sqrt{x'^2 + y'^2 + h'^2} \tag{10}$$

where λ is the scale or speed factor. It follows then that

$$\lambda = \frac{v_\mathrm{t}}{\sqrt{x'^2 + y'^2 + h'^2}} \tag{11}$$

The optimization variables are then the aircraft initial and final jerks and τ_f such that the optimization variable vector is $\Xi = [x'''_{0,f}, y'''_{0,f}, h'''_{0,f}, v''_{0,f}, \tau_f]$.

For the generation of trajectories involving climb, cruise and descent phases, the trajectory was treated as a series of maneuvers. Therefore, to improve the accuracy of the optimization, three piecewise polynomial trajectories $(\mathcal{P}1, \mathcal{P}2, \mathcal{P}3)$ were optimized, where the end states of one polynomial determined the initial conditions for the next such that

$$\mathbf{r}(\tau) = \begin{cases} \mathbf{r}_{\mathcal{P}1}(\tau), & \tau \in [\tau_o, \tau_1] \\ \mathbf{r}_{\mathcal{P}2}(\tau), & \tau \in [\tau_1, \tau_2] \\ \mathbf{r}_{\mathcal{P}3}(\tau), & \tau \in [\tau_2, \tau_f] \end{cases} \tag{12}$$

and where the optimization variables became

$$\Xi = \begin{bmatrix} x'''_0, y'''_0, h'''_0, v''_0, \\ x_1, y_1, h_1, x'_1, y'_1, h'_1, x''_1, y''_1, h''_1, x'''_1, y'''_1, h'''_1, v''_1, \\ x_2, y_2, h_2, x'_2, y'_2, h'_2, x''_2, y''_2, h''_2, x'''_2, y'''_2, h'''_2, v''_2, \\ x'''_f, y'''_f, h'''_f, v''_f, \\ \tau_1, \tau_2, \tau_f \end{bmatrix} \tag{13}$$

Conversion between the time and arc derivatives is achieved by

$$\begin{aligned} \dot{r} &= \lambda r'; \\ \ddot{r} &= \lambda(r''\lambda + r'\lambda') \\ \dddot{r} &= \lambda^3 r''' + 3\lambda^2\lambda' r'' + (\lambda^2 + \lambda\lambda'^2)r' \end{aligned} \tag{14}$$

The ground speed v_g is given as $v_g = \sqrt{(\dot{x}_\mathrm{a} + w_x)^2 + (\dot{y}_\mathrm{a} + w_y)^2}$, where the wind speeds in the 3 coordinate directions are w_x, w_y and w_h. The subscripts $_\mathrm{a}$ and $_\mathrm{i}$ designate the air mass and the inertial frames respectively.

The time t is calculated from the following relationship

$$t = \int \frac{1}{\lambda} d\tau \tag{15}$$

To transform the polynomials to the system dynamics, a point mass model is used. Therefore the states and controls are determined by inverting the following equations,

$$\begin{aligned} \dot{x}_\mathrm{i} &= v_\mathrm{t}\cos\gamma_\mathrm{a}\cos\chi_\mathrm{a} + w_x, & \dot{v}_\mathrm{t} &= \frac{T - D}{m} - g\sin\gamma_\mathrm{a} \\ \dot{y}_\mathrm{i} &= v_\mathrm{t}\sin\chi_\mathrm{a}\cos\gamma_\mathrm{a} + w_y, & \dot{\chi}_\mathrm{a} &= \frac{gn\sin\phi}{v_\mathrm{t}\cos\gamma_\mathrm{a}} \\ \dot{h}_\mathrm{i} &= v_\mathrm{t}\sin\gamma_\mathrm{a} + w_h, & \dot{\gamma}_\mathrm{a} &= \frac{g}{v_\mathrm{t}}(n\cos\phi - \cos\gamma_\mathrm{a}) \end{aligned} \tag{16}$$

The flight path angle is $\gamma(t)$ and $\chi(t)$ is the heading angle. The aircraft controls are $\mathbf{U}(t) = [T(t), n(t), \phi(t)]^T$, where $T(t)$ is thrust, $n(t)$ is load factor and $\phi(t)$ is the bank angle. The drag D is modelled with the aid of the BADA drag polars [21], aircraft mass is m, g is gravitational acceleration. As in [26],

the wind's impact on velocity and path are considered but not its impact on acceleration.

Therefore, through inverse dynamics, the state and control vectors are expressed as functions of the output trajectory vector $\mathbf{r}$ and its derivatives such that

$$\mathbf{X} = \mathbf{f}_X(\mathbf{r}, \dot{\mathbf{r}}, \ddot{\mathbf{r}} \ldots), \qquad \mathbf{U} = \mathbf{f}_U(\mathbf{r}, \dot{\mathbf{r}}, \ddot{\mathbf{r}} \ldots) \tag{17}$$

Once the state and control histories are determined, constraints may be applied to ensure that values lie between defined limits

$$\begin{aligned} x \in [x_{min}, x_{max}], \qquad & y \in [y_{min}, y_{max}] \\ h \in [h_{min}, h_{max}], \qquad & T \in [T_{min}; T_{max}] \\ n \in [n_{min}; n_{max}], \qquad & |\phi| \leq |\phi_{max}| \\ v_{CAS} \in [v_{min_{CAS}}; v_{max_{CAS}}], \qquad & v_{\mathrm{t}} \in [v_{\mathrm{t}_{min}}; v_{\mathrm{t}_{max}}] \\ \gamma_{\mathrm{i}} \in [\gamma_{\mathrm{i}_{min}}; \gamma_{\mathrm{i}_{max}}], \qquad & \chi_{\mathrm{i}} \in [\chi_{\mathrm{i}_{min}}; \chi_{\mathrm{i}_{max}}] \\ |a_n| \leq |a_{n_{max}}| & \end{aligned} \tag{18}$$

where the positional and angle constraints on x, y, h, γ and χ are user defined and scenario specific. The constraints on roll angle $|\phi_{max}|$, longitudinal acceleration $|a_{l_{max}}|$ and normal acceleration $|a_{n_{max}}|$ are defined by the BADA dynamics model [21]. The speed constraints $v_{min_{CAS}}$, defined in Calibrated Air Speed (CAS) and the thrust constraint $T_{min,max}$ are determined from BADA functions [21]. Waypoint constraints were also used to approximate ATM constraints imposed by airspace sectorization, procedures and traffic flow corridors, and are covered in detail in [24].

Therefore, where $\mathbf{c}$ represents the trajectory constraint violations, the optimal control problem can then be treated as an NLP problem in the form

$$\min_{\Xi} J(\mathbf{X}, \mathbf{U}), \quad s.t. \quad \mathbf{c}(\mathbf{X}, \mathbf{U}) \leq 0 \quad \mathbf{c} \in \mathbb{R}^M \tag{19}$$

where the trajectory search is conducted in the output space and only the algebraic equations need to be solved.

The NLP problem was then solved using the Differential Evolution (DE) stochastic optimization method. DE is an open standard evolutionary algorithm that has already been used successfully with the IDVD method [27], [24]. From a set of initial parameter values, DE uses a process of mutation, combination and selection to find optimization variables that lower the objective function value until no further improvements in the objective can be found. The IDVD-DE method has been used in this paper to generate fuel efficient but not fuel optimal trajectories.

III. Use level segments to define vertical fuel inefficiency

To achieve a zero inefficiency 3Di score for the climb phase of flight, NATS recommend that departing aircraft perform a Continuous Climb Departure (CCD), which is then facilitated by the ANSP from an air traffic control perspective [19]. CCDs involve giving the aircraft a direct uninterrupted routing to the top of climb. However the current guidance can encourage continuous gains in height over gains in speed, which may result in aircraft achieving less fuel efficient climbs. To demonstrate, an example simulation was performed. The simulation scenario consisted of an A321 climb to a RFL of 6,705m/22,000ft at a specified distance from take-off. Three trajectories solutions were investigated, a standard BADA speed schedule climb to the RFL followed by a level cruise to the target distance, a constant angle/constant acceleration climb to the target distance and an IDVD-DE generated trajectory to the target distance. The common start and end speeds for all trajectories were taken from the BADA speed schedule. However, to provide the clearest illustration of the differences between the trajectories, the operational 129ms^{-1}/250kts IAS constraint below 3,048m/10,000ft was not enforced.

From Fig. 1, examining the BADA generated trajectory solution, it can be seen that the aircraft climbs at approximately 90% maximum climb thrust using the standard BADA speed schedule directly to the RFL. On reaching the RFL, the aircraft sets thrust equal to drag for the remaining time to the target distance.

For the constant angle climb solution, a constant acceleration, and therefore a linear speed profile climb as proposed in [14] is utilised. Aircraft thrust is determined inversely to deliver the desired dynamics. The speed schedule, although low relative to the other trajectories did not violate the minimum speed constraint.

After an initial climb out common to all solutions, the trajectory generated by the IDVD-DE method consists of a level segment at low flight levels followed by a fast climb to the target conditions. The level segment is used principally to accelerate the aircraft using excess thrust. Although fuel burn is expensive at lower flight levels, the low level acceleration is utilised to achieve a faster, more direct climb to the target conditions. It can be seen from the thrust profile that the thrust utilised is limited by the BADA acceleration constraint and that this requires the thrust to be reduced during acceleration before higher levels are reintroduced when the flight recommences the climb at higher speeds.

Of the 3 trajectories, the IDVD-DE method had both the shortest flight time and the lowest fuel burn 1,265kg/807sec. The next lowest fuel burn was provided by the BADA trajectory, which had the next shortest flight time, 1,376kg/843sec. The constant acceleration climb trajectory had the longest flight time and was also the trajectory with the largest fuel burn, 1,458kg/1,046sec. While the trajectories presented above are considered to be operationally achievable they are unlikely to be operationally desirable. They do however illustrate the importance of speed management in delivering a fuel efficient climb trajectory. Therefore the results suggest that fuel efficient climbs are achieved by prioritising energy management and not by exclusively focusing on continuously climbing the aircraft.

Examining the trajectory solutions relative to the 3Di score, the BADA and the constant angle climb trajectories would have 3Di scores of zero inefficiency due to neither trajectory having a level flight segment below the RFL. This is despite there being considerable differences in the fuel burn for both those solutions. The IDVD-DE method generated the most fuel efficient trajectory, but would have been graded by the 3Di score as being the least fuel efficient trajectory, as the trajectory has a level segment of flight at low flight levels.

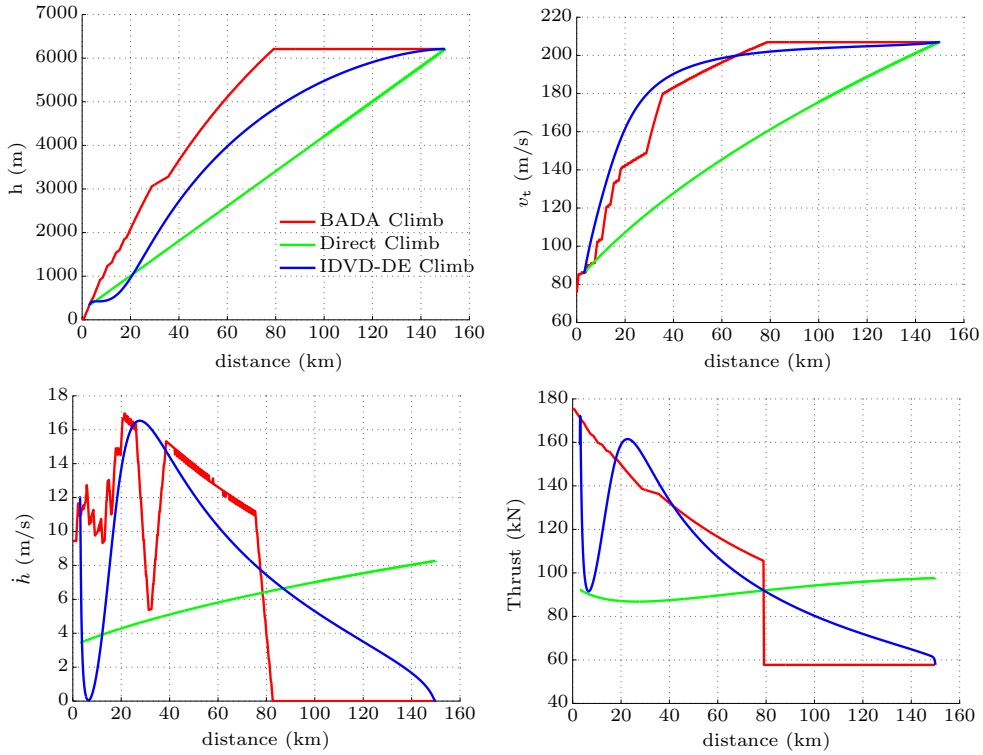

Fig. 1. Climb profile comparisons

IV. Optimum vertical profile

In the 3Di score calculation, BADA vertical trajectories are assumed to define the theoretical optimum trajectory. To examine the fuel efficiency of a BADA generated trajectory, a simulation scenario was created comparing an IDVD-DE generated trajectory to a BADA generated trajectory. For the scenario, the 3Di demonstration flight was used for reference [28], [16]. The demonstration flight involved an uninterrupted A321 flight from London to Edinburgh, unconstrained by typical ATM constraints and with a cruising height of 10,363m/34,000ft [28], [16]. Therefore a scenario was setup involving an A321 flight for a great circle distance equivalent to the Heathrow to Edinburgh distance (544km). The BADA trajectory used for comparison with the IDVD-DE method was generated by the BADA performance calculation tool, with a specified cruise height set to 10,363m/34,000ft. The input boundary values for the IDVD-DE method were also defined by the BADA solution.

Comparing the IDVD-DE trajectory to the BADA generated trajectory in Fig. 2, it can be seen that during the departure climb phase that the IDVD-DE solution has a shallow near level acceleration segment at a height of approximately 1,000m. The shallow segment was used to accelerate the aircraft, with much of the gain in kinetic energy then used to increase the climb rate of the aircraft. Higher levels of thrust are then re-introduced to maintain the high climb rate at the higher speeds. This results in the IDVD-DE trajectory having a faster initial climb out relative to the BADA trajectory, but requires the IDVD-DE trajectory to use maximum climb thrust where the BADA trajectory uses a derated thrust of 90% maximum climb thrust. Higher in the climb phase, the thrust is reduced and used preferentially for climbing while the speed is allowed to level out. However, the IDVD-DE solution is then required to perform a second acceleration segment so that it does not violate the BADA defined minimum speed constraint, shown in orange in Fig. 2. The IDVD-DE trajectory reaches a maximum cruise height of 10,973m/36,000ft before commencing a shallower, slower descent than the BADA trajectory until below 3,048m/10,000ft, after which both trajectories assume a 3 degree descent slope to final approach.

At 2,176kg of fuel, the IDVD-DE generated trajectory used almost 10% less fuel than the 2,412kg of fuel used by the BADA trajectory. Therefore, the results suggest that the BADA trajectories used in the calculation of the 3Di score are not fuel or CO2 optimal trajectories. It can be seen that IDVD-DE trajectory cruised at a slower more economical speed than the BADA trajectory, having a longer flight time of 50 minutes relative to the BADA trajectory flight time of 43 minutes. However, airlines normally fly the aircraft using a cost index that is a balance between the fuel burn cost and the operating time cost of the aircraft. It can also be seen that the IDVD-DE trajectory involved an extended use of maximum available climb thrust on climb out. Airlines usually prefer to minimise the use of maximum thrust levels due to the wear and tear it causes on the engine. Therefore the results highlight that the most fuel/CO2 efficient trajectory may not be the user preferred trajectory. The results also highlighted that it is likely that there is a trade-off between fuel burn and maintenance costs. It is suggested that a multiobjective trajectory optimization study, could be used to investigate the trade-offs between trajectories optimized for fuel, operating and maintenance costs.

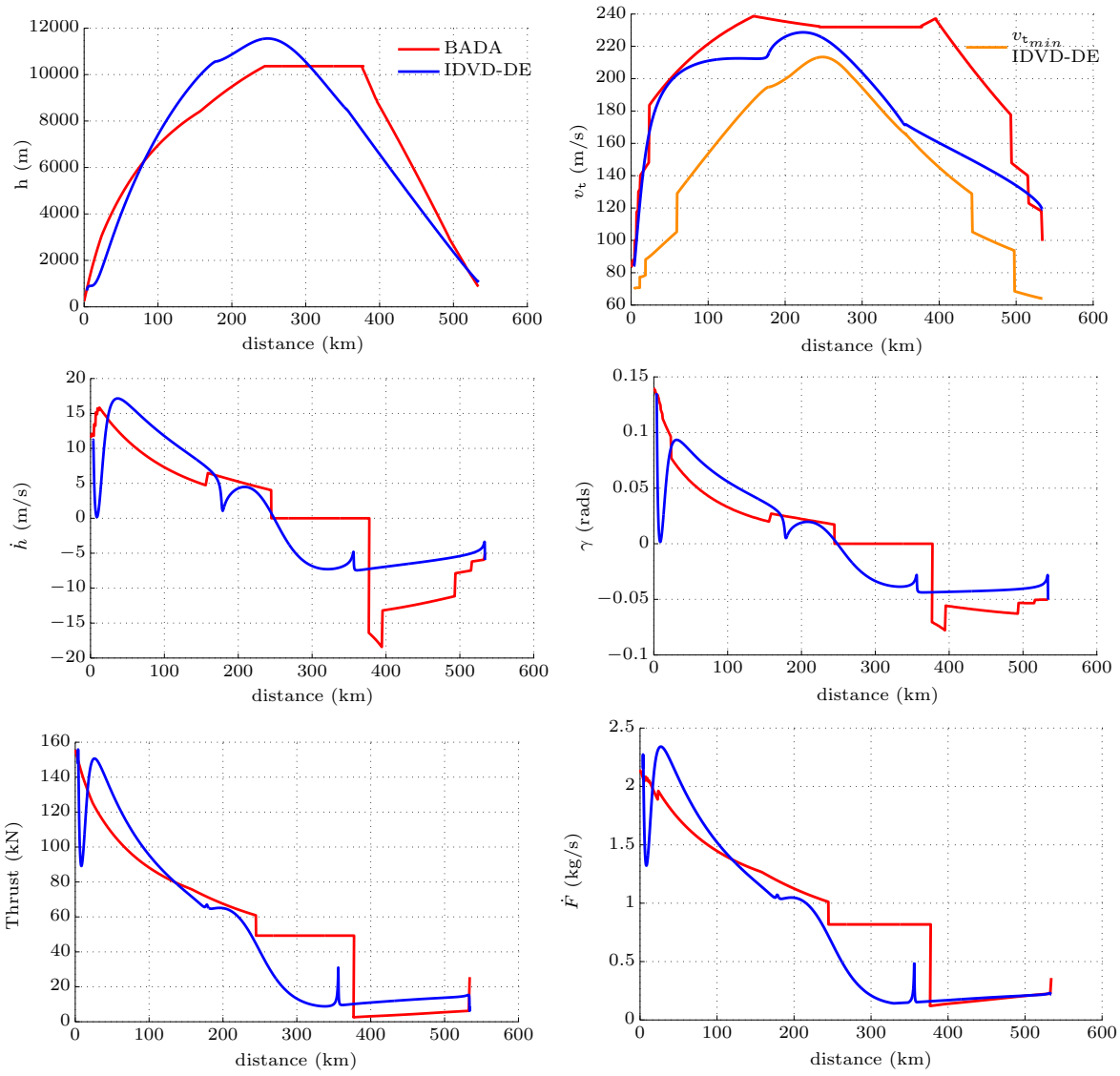

Fig. 2. Fuel efficient trajectory comparisons

V. Flight Planning Constraints

To demonstrate the impact of flight planning constraints on a preferred trajectory, the IDVD-DE method was used to generate procedurally constrained and unconstrained fuel efficient trajectories for a representative flight from London Gatwick (EGKK) to Paris Charles de Gaule (LFPG). The fuel inefficiency introduced by the constraints was then analysed with consideration of the 3Di score. The flight plan generated from [29], required the constrained trajectory to follow the Hardy SID from Gatwick, The UM605 airway from Hardy to the DPE and to descend on the DPE 4W STAR towards Paris. The trajectory waypoint constraints for the constrained trajectory are shown in Table I.

The waypoint constraints were taken from the relevant AIP and SID/STAR charts. From the DPE STAR chart, there was an additional below 144ms^{-1}/280kts IAS constraint at DPE, however it was found that this constraint conflicted with the minimum BADA defined flight speed constraint at the DPE constraint target height of 6,401m/22,000ft. Therefore, the constraint was removed for this study. A corridor constraint [30] was considered to represent the UM605 airway, however it was found that the waypoint constrained trajectory pre-satisfied the airway constraint and therefore the corridor constraint is not shown here. In addition to the waypoint constraints the constrained trajectory was also subject to the 129ms^{-1}/250kts IAS below 3,048m/10,000ft rule. Both trajectories were required to be established in line with the runway on final approach by 6 DME and to fly three degree descending approaches on the ILS below 1,036m/3,400ft.

Fig. 3 and Fig. 4 show the constrained and unconstrained trajectory solutions to the London-Paris scenario where the height and speed profiles are shown relative to the circular waypoint crossing and the cylindrical height and speed constraints. Comparing the solutions in Fig. 3 and Fig. 4, it can be seen clearly that, close to Gatwick, there are large differences between the speed profiles of the two trajectories.

TABLE I. FLIGHT PLANNING CONSTRAINTS

Waypoint	Lat	Long	Diameter (m)	H (m)	H tolerance	V (m/s)	V tolerance
MIDD10	51.128	-0.358	5000	1220	460	-	-
OCKD13	51.088	-0.428	5000	1297	383	-	-
OCKD18	51.005	-0.421	5000	1525	155	-	-
OCKD23	50.923	-0.415	5000	1846	166	-	-
OCKD28	50.84	-0.409	5000	-	-	-	-
BOGNA	50.702	-0.252	10000	-	-	-	-
HARDY	50.473	0.485	10000	-	-	-	-
DPE	49.923	1.171	5000	6401	153	-	-
SOKMU	49.334	1.419	5000	3962	152	-	-
MEURE	49.301	1.851	10000	2743	153	129	5

The unconstrained trajectory is not constrained by the less than 129ms^{-1}/250kts bellow 3,048m/10,000ft restriction, nor the HARDY SID constraints, therefore, thrust is initially applied to preferentially increase aircraft speed at lower flight levels leading to a faster climb to higher flight levels. When the aircraft reaches a height of approximately 6,000m, it begins to trade-off some of its speed for continued gains in height. The constrained trajectory solution climbs from EGKK following the HARDY SID restrictions. At 3,048m/10,000ft the aircraft clears the 129ms^{-1}/250kts IAS speed restriction and begins an acceleration to 200ms^{-1}/390kts while also continuing to climb. Once the aircraft in the constrained solution nears its cruise height, it also begins to trade-off some of its speed for continued gains in height.

Examining the descent from cruise, it can be seen that the unconstrained trajectory, unconstrained by the DPE STAR, begins its descent to Paris earlier than the constrained trajectory. It assumes a shorter path to LFPG, reducing speed early, helping it to minimise fuel burn. For the constrained solution, the aircraft must stay higher for longer due to the STAR constraints. However, once the aircraft does commence its descent, it quickly assumes similar descent rates, speed and fuel consumption profiles as those of the unconstrained trajectory.

In terms of fuel burn, the ATM constraints considered introduced a 321kg/17% fuel inefficiency relative to the unconstrained trajectory solution. Analysing the results relative to the 3Di score, it is reasonably expected that the path extension factor σ would account for horizontal path inefficiencies introduced by the constraints. However, for the vertical efficiency, it is clear that the ATM constraints alter the most efficient cruising height and therefore the cruising height requested by an airline in the flight plan. Therefore, there is an RFL related fuel inefficiency included in the flight plan submitted to the ANSP.

As inefficiencies in the RFL are not considered in the the calculation of the 3Di score, the constraints have introduced a vertical inefficiency into the trajectory that is not quantified by the metric. The results also showed that including the waypoint constraints in the flight planning caused them to be navigated with no periods of level flight. So, similar to the RFL inefficiency, the vertical fuel inefficiency related to those waypoints is again unquantified by the 3Di score.

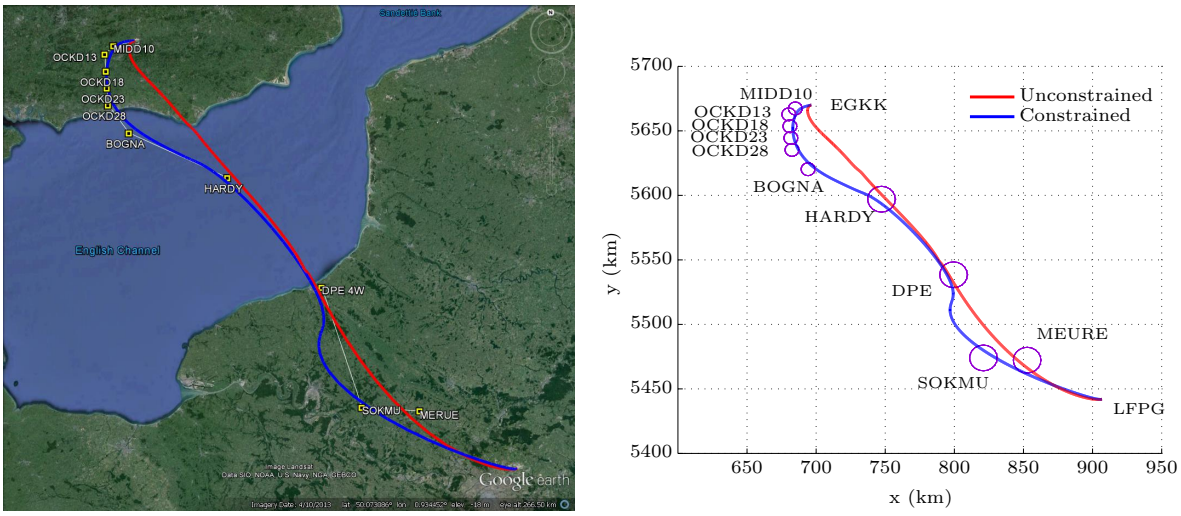

Fig. 3. London-Paris constrained and unconstrained trajectory solutions

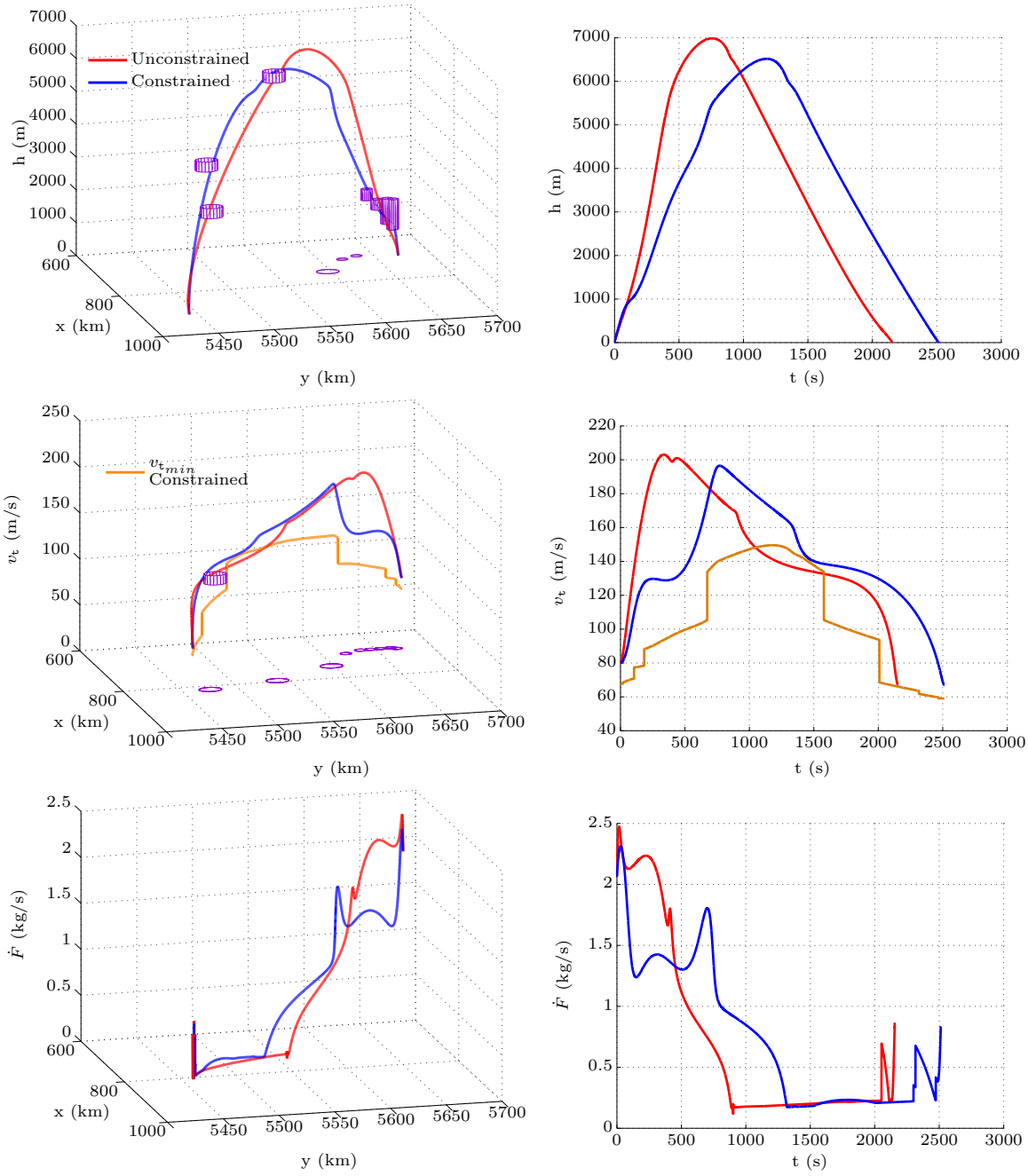

Fig. 4. London-Paris constrained and unconstrained trajectory solutions

VI. Conclusion

In response to a Eurocontrol review of the metric, the 3Di score has been analysed using a trajectory optimization method based on optimal control.

The results suggest that further development is required for the metric to be considered as a flight or fuel efficiency metric. The results show that BADA trajectories used in the 3Di score to define the optimum fuel efficient operation of the aircraft are not optimal fuel efficient trajectories. The results also highlight the importance of considering flight planning restrictions when calculating the fuel inefficiency of a trajectory.

The fuel efficiency of a flight trajectory is a collaboration between the flight crew and ATC. Separating ATM introduced fuel inefficiencies from operator introduced inefficiencies is a subject that still requires further research. However, the ANSP has significant influence over trajectory height, speed and climb rates through tactical instructions and the design of the ATM system, including climb and descent procedures and standing agreements, and also through the guidance it issues on efficient climb and descent operations. The results have shown that currently the 3Di score is insensitive to a wide number of operational changes that can be applied to the vertical trajectory to reduce the fuel burn of a flight. Therefore, if as proposed in [18], the 3Di score is to drive long term operational improvements in fuel related trajectory operations,

the metric should be sensitive to operational changes in the vertical trajectory that significantly impact fuel consumption, and not solely be sensitive to periods of level flight away from a BADA trajectory.

ICAO defines 3 prominent types of aviation related environmental impacts as climate changing emissions, air quality emissions and noise. It is well established that there are a wide number of trade-offs between the objectives. particularly for noise objectives, which are very sensitive to local conditions. In CO2, the 3Di score only attempts to look at the inefficiencies related to one form of environmental impact. Also results here have shown that the BADA trajectory used to benchmark the inefficiencies of flown trajectories is not a CO2 optimal trajectory. Defining a environmentally efficient trajectory is likely to involve a trade-off analysis between the competing environmental objectives [24].

The results in this paper offer a preliminary analysis of the 3Di score using a trajectory optimization method. The results must still be confirmed by further simulation results, potentially using more accurate trajectory optimization methods. Further consideration must also be given to the impact of wind, aircraft weight, flight planning restrictions, environmental trade-offs and airline operating costs when defining reference trajectories intended to benchmark inefficiencies in flown trajectories.

REFERENCES

[1] Airbus, "Flying on demand: Global market forecast 2014-2033," 2014.

[2] SESAR Joint Undertaking, "European ATM master plan, edition 2," 2012.

[3] International Civil Aviation Organization, "Environmental report 2013," 2013.

[4] S. K. Ribeiro, S. Kobayashi, M. Beuthe, J. Gasca, D. Greene, D. S. Lee, Y. Muromachi, P. J. Newton, S. Plotkin, D. Sperling *et al.*, "Transportation and its infrastructure," *Institute of Transportation Studies*, 2007.

[5] European Federation for Transport and Environment, "Grounded: How ICAO failed to tackle aviation and climate change and what should happen now," 2010.

[6] M. Grote, I. Williams, and J. Preston, "Direct carbon dioxide emissions from civil aircraft," *Atmospheric Environment*, vol. 95, pp. 214–224, 2014.

[7] International Civil Aviation Organization, "Environmental report 2010," 2010.

[8] European Commission, "The EU Emissions Trading System EU ETS factsheet," http://ec.europa.eu/clima/publications/docs/factsheet_ets_en.pdf/, 10 2014.

[9] International Civil Aviation Organization, "ICAO Assembly Resolution A38-18: Consolidated statement of continuing ICAO policies and practices related to environmental protection Climate change," 4 October 2013.

[10] ——, "Doc. 10018, Report of the assessment of market-based measures," 2013.

[11] Advisory Council Aeronautics Research in Europe, "Strategic Research Agenda. Volume 1," September 2012.

[12] ——, "Strategic Research Agenda. Volume 2," September 2012.

[13] G. Horton, "Future aircraft fuel efficiencies - final report," UK Department for Transport, 2010.

[14] SESAR Joint Undertaking, "SESAR and the environment," 2010.

[15] UK Civil Aviation Authority, "Consultation on NATS (En Route) plc (NERL) flight efficiency performance regime," https://www.caa.co.uk/docs/5/Flight%20efficiency%20consultation%20-letter%2002082011.pdf, 02 2011.

[16] C. Nutt, "OA 1161 Version 1.3, NATS Fuel efficiency metric," 2012.

[17] S. Hammond, J. Civil, M. Ross, and K. Slater, "Air traffic control, business regulation and CO2 emissions," *OR insight*, vol. 25, no. 3, pp. 127–149, 2012.

[18] NATS, "Environmental performance," http://www.nats.aero/environment/3di/, 11 2014.

[19] ——, "3Di environmental performance measure," http://www.nats.aero/wp-content/uploads/2012/07/3di_Infocard.pdf, 07 2012.

[20] ——, "NATS records airspace efficiency improvement in 2013," http://www.nats.aero/news/nats-records-airspace-efficiency-improvement-2013/, 03 2014.

[21] A. Nuic, "User manual for the Base of Aircraft Data (BADA) revision 3.10," 2012.

[22] Eurocontrol, "Eurocontrol response, consultation on NATS (En Route) plc (NERL) flight efficiency performance regime," https://www.caa.co.uk/docs/5/20111013%20Eurocontrol.pdf, 10 2011.

[23] O. Yakimenko, "Direct method for rapid prototyping of near-optimal aircraft trajectories," *AIAA Journal of Guidance, Control, and Dynamics*, vol. 23, no. 5, 2000.

[24] Q. McEnteggart and J. Whidborne, "A multiobjective trajectory optimisation method for planning environmentally efficient trajectories," in *2012 UKACC International Conference on Control*. IEEE, 2012, pp. 128–135.

[25] C. Lai and J. Whidborne, "Real-time trajectory generation for collision avoidance with obstacle uncertainty," in *AIAA Guidance, Navigation and Control Conference, AIAA 2011-6598*, Portland OR, August 2011.

[26] W. Glover and J. Lygeros, "A stochastic hybrid model for air traffic control simulation," in *Hybrid Systems: Computation and Control*. Springer, 2004, pp. 372–386.

[27] R. Drury, *Trajectory Generation for Autonomous Unmanned Aircraft Using Inverse Dynamics*. PhD Thesis Cranfield University, 2010.

[28] NATS, "NATS, British Airways and BAA in UK-first with perfect flight," http://www.nats.aero/news/nats-british-airways-and-baa-in-uk-first-with-perfect-flight/, 07 2010.

[29] RouteFinder, "Route generator for PC flight simulation use," http://rfinder.asalink.net/free/.

[30] D. Mellinger and V. Kumar, "Minimum snap trajectory generation and control for quadrotors," in *Robotics and Automation (ICRA), 2011 IEEE International Conference on*. IEEE, 2011, pp. 2520–2525.